Optical properties of reflective liquid crystal polarization volume gratings

Yun-Han Lee,[1,†] Ziqian He,[1,†] and Shin-Tson Wu[1,*]

[1]College of Optics & Photonics, University of Central Florida, Orlando, Florida 32816, USA
*Corresponding author: swu@creol.ucf.edu

Polarization volume gratings are self-organized liquid crystal helical structures. They exhibit high diffraction efficiency and unique polarization selectivity. In this work, we investigate and compare two different configurations of polarization volume gratings: planar and slanted structures. We present the optical properties of polarization volume gratings with emphasis on their polarizing nature. Further experimental results reveal the existence of the slanted configuration.   © 2019 Optical Society of America

https://doi.org/10.1364/JOSAB.36.0000D9

1. INTRODUCTION

The emerging see-through near-eye displays, such as augmented reality and mixed reality, have inspired new applications of optical gratings as waveguide-coupling components [1,2]. Among them, reflective polarization volume gratings (PVGs) based on self-organized cholesteric liquid crystals (CLCs) are a strong contender [3–5]. Different from the established surface-relief gratings and volume Bragg gratings (holographic gratings) [6–8], the modulation of PVGs is based on the spatially distributed optical axis of *anisotropic* liquid crystals (LCs), while the other two are based on the spatially distributed refractive index of *isotropic* materials. Such a difference gives rise to the unique polarization sensitivity of PVGs, and yet the polarizing properties of PVGs have not been thoroughly investigated.

In this work, we investigate the optical properties of two different types of reflective PVGs categorized by their axis distribution: planar PVGs and slanted PVGs. Planar PVGs, as shown in Fig. 1(a), have a helical axis perpendicular to the substrate, and the tilt angle of LC directors is zero across the structure. The previously demonstrated PVGs belong to this category, and yet the other configuration, as shown in Fig. 1(b), is also possible. We refer to this orientation profile as slanted PVGs (or slanted CLCs), exhibiting uniform molecular rotation with respect to a slanted helical axis. In the following sections, we will explore and discuss the differences in their optical properties. Further experiments prove the existence of the slanted configuration.

2. METHODS

For clarity, we define the horizontal periodicity (P_x) as the distance by which LC director rotates 180° along the horizontal direction, and vertical periodicity (P_y) as the distance by which

LC director rotates 180° along the vertical direction. The Bragg periodicity (P_B) is related to P_x and P_y as follows:

$$\frac{1}{P_x^2} + \frac{1}{P_y^2} = \frac{1}{P_B^2}, \tag{1}$$

where the slant angle, ϕ, is related to P_x and P_y as follows:

$$\tan \phi = \frac{P_y}{P_x}. \tag{2}$$

The corresponding Bragg wavelength can then be described as

$$\lambda_B = 2nP_B \cos \phi, \tag{3}$$

where n is the average refractive index of the employed LC. All above definitions work for both LC configurations depicted in Fig. 1.

The PVGs in this work were fabricated in the following steps [5]. A thin layer (∼10 nm) of photoalignment material brilliant yellow [9] was spin-coated onto a cleaned glass slide, and then exposed with two coherent circularly polarized laser beams ($\lambda = 457$ nm) with opposite handedness. The two beams were aligned at an angle of 31.3° to the normal of the substrate in a symmetric configuration (i.e., 62.6° between two beams). This generated a polarization interference pattern with a horizontal periodicity $P_x = 440$ nm. The LC precursor consisted of 2.3 wt. % R5011 as a chiral agent to induce self-organized helical structure, 3.0 wt. % Irgacure 651 as a photo-initiator to accelerate the UV curing process, and 94.7 wt. % RM257 as a photocurable LC polymer. The precursor was dissolved in toluene and spin-coated onto the exposed brilliant yellow photoalignment layer. A 365-nm UV light was applied to cure the reactive mesogen until a sufficient film thickness was obtained. For a thin PVG (<2.0 µm), either coating once
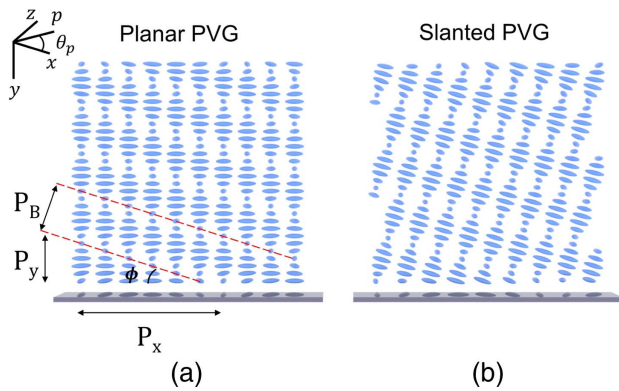
Fig. 1. LC director profile of (a) planar PVG and (b) slanted PVG. θ_p is defined as the angle of the linear polarizer.

Fig. 2. (a) Optical efficiency of PVGs as a function of film thickness; (b) Stokes parameters S_3 as a function of film thickness. Solid line, slanted PVGs; dashed line, planar PVGs.

or multiple times can work, but for a thick PVG, coating multiple times is recommended.

To characterize the polarization properties, the PVG was fixed on a rotation stage and set to the center of a glass cylinder that contains index matching oil ($n = 1.58$). The incident light was perpendicular to the PVG at the initial state. The angle of incidence (in the x-y plane) can then be adjusted by rotating the PVG, and the Stokes parameter S_3 of the diffracted beam was directly measured by a polarimeter (PAX100VIS, Thorlabs). The efficiency is defined as the intensity of the diffracted beam to that of the reference beam passing through the glass cylinder with index matching oil only (without PVGs), and the transmittance measurements were also normalized to the same condition.

The simulation of PVGs was carried out with the finite-element method [3] using the following parameters unless otherwise stated: the horizontal periodicity $P_x = 440$ nm and the vertical periodicity $P_y = 205$ nm; the helical chirality was right-handed; the average refractive index of the LC material was 1.58; the refractive index of surrounding materials was 1.58; the LC birefringence was 0.15; the probing wavelength was 532 nm; and the input light was right-handed circularly polarized.

3. RESULTS AND DISCUSSION

First, we simulated the optical efficiency and polarizing properties of these two reflective PVG configurations. In Fig. 2(a), as expected from a reflective Bragg grating, the increasing film thickness leads to an increased diffraction efficiency. The growth trend is very similar between the planar (dashed lines) and slanted (solid lines) PVGs. To investigate the polarization property of the diffracted light, we use Stokes parameter S_3 as an indicator. S_3 denotes the degree of circular polarization of light. For example, $S_3 = 1$ means right-handed circularly polarized light, while $S_3 = -1$ stands for left-handed circularly polarized light. As Fig. 2(b) shows, there exist drastic differences in S_3 between these two PVGs. Although both decrease as the film thickness increases, the slanted PVG (solid lines) has a much higher S_3 at near unity, indicating that the diffracted light is nearly circularly polarized. On the other hand, the diffracted light from the planar PVG significantly
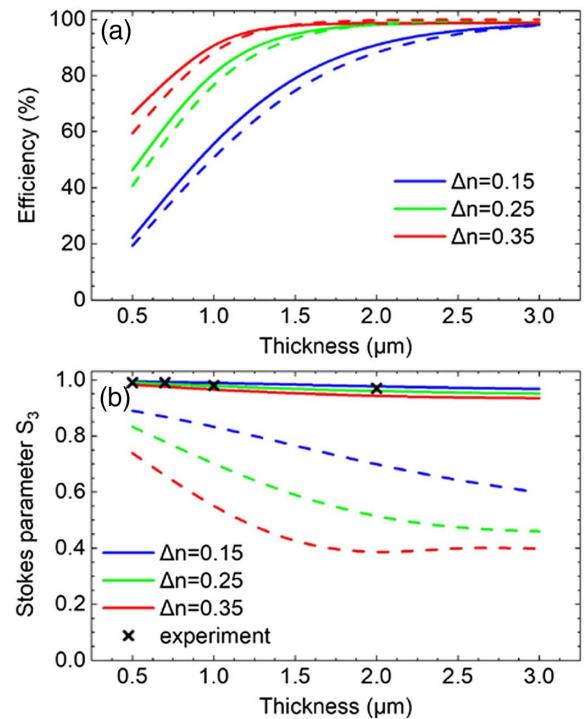
deviates from the circular polarization. To validate these predictions, in experiment we fabricated four samples with different thicknesses. The experimental results, denoted as crosses in Fig. 2(b), agree very well with the simulation results of slanted PVGs. This is different from the previously reported result for large slanted angle ϕ [10], and therefore indicates that when ϕ is appropriate ($\sim 25°$ in our experiment), the minimized free energy prefers a slanted PVG structure as opposed to planar. The PVG fabricated in this manner can be approximated as a diffractive circular polarizer.

The simulated grating efficiency for different input polarization states is depicted in Fig. 3, with a film thickness of 2.0 μm. The input polarization states are expressed using the Jones matrix in local coordinate as

$$J = \begin{bmatrix} \cos \alpha \\ \sin \alpha \times e^{i\beta} \end{bmatrix}, \tag{4}$$

where α and β are the phase angles of the polarization state.

From Fig. 3, both planar PVGs [Fig. 3(a)] and slanted PVGs [Fig. 3(b)] have minimal efficiency near left-handed circularly polarized input ($\alpha = 45°$, $\beta = 270°$) and highest efficiency near right-handed circularly polarized input ($\alpha = 45°$, $\beta = 90°$), as denoted by the crosses in the figures. However, it is noteworthy that the input polarization states at the highest and the lowest efficiency for the slanted PVG slightly deviate from the circular polarization states, resulting in asymmetric efficiency for a linearly polarized input light. This suggests that slanted PVGs are sensitive to the polarization angle of a linearly polarized input light, while planar PVGs are not.
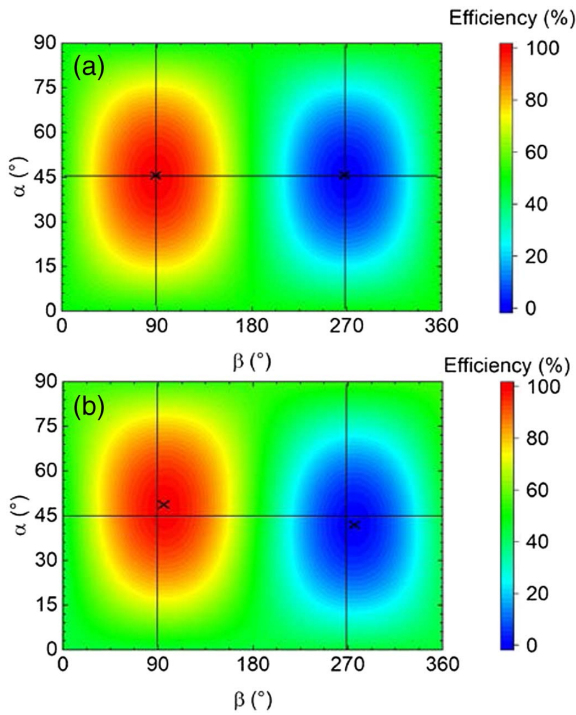
Fig. 3. Normalized grating efficiency for different input polarization states [expressed by α and β as defined in Eq. (4)] for (a) planar PVGs and (b) slanted PVGs. Film thickness, 2.0 µm.

Fig. 5. Simulated wavelength-dependent optical efficiency (black curves) and S_3 (red curves) of (a) a planar PVG and (b) a slanted PVG. Film thickness, 2.0 µm.

To validate this, we simulate the transmittance variations as a function of input linear polarization angle for both configurations, and results are depicted in Fig. 4. Due to the asymmetry found in Fig. 3, the transmission of a slanted PVG is sensitive to the input polarization angle, while the planar PVG is rather insensitive. In experiment, the grating transmittance was measured as a function of the input polarizer angle (defined as θ_p in Fig. 1). A 2.0-µm PVG sample was applied, and a rotatable linear polarizer was placed in front of an unpolarized 532-nm laser beam. Good agreement is found between experiment and simulation for a slanted PVG. This again confirms the PVG fabricated following this method manifests a slanted structure. This measurement can serve as a simple method to differentiate slanted and planar PVGs.
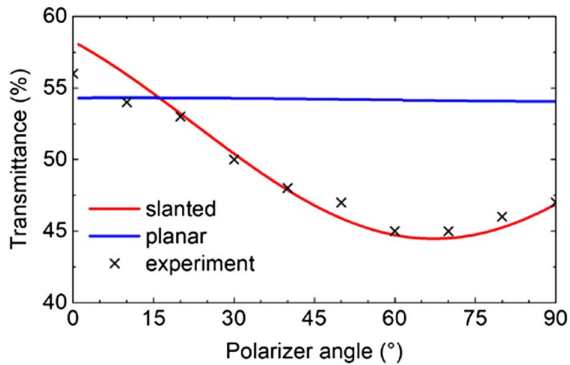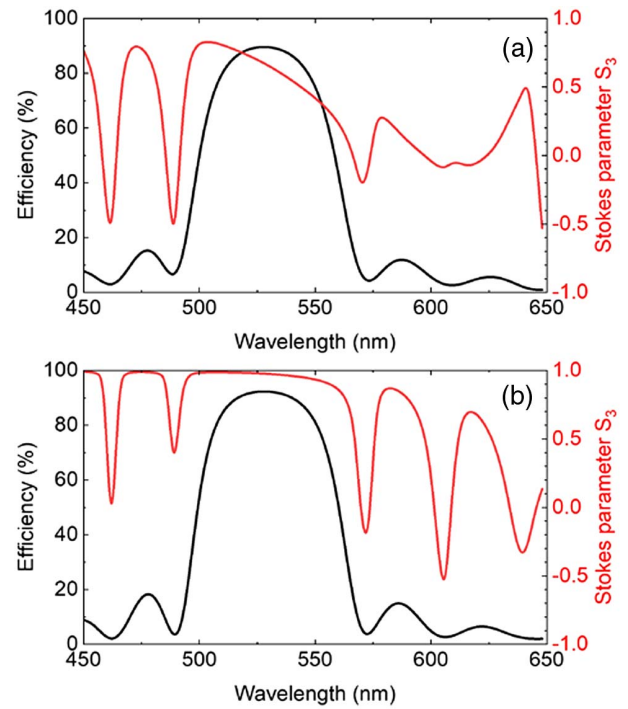
The spectral behavior of optical efficiency and S_3 are further investigated for slanted and planar PVGs, as shown in Fig. 5. As designed, the central wavelength peaks at 532 nm at normal incidence. By comparing the results shown in Figs. 5(a) and
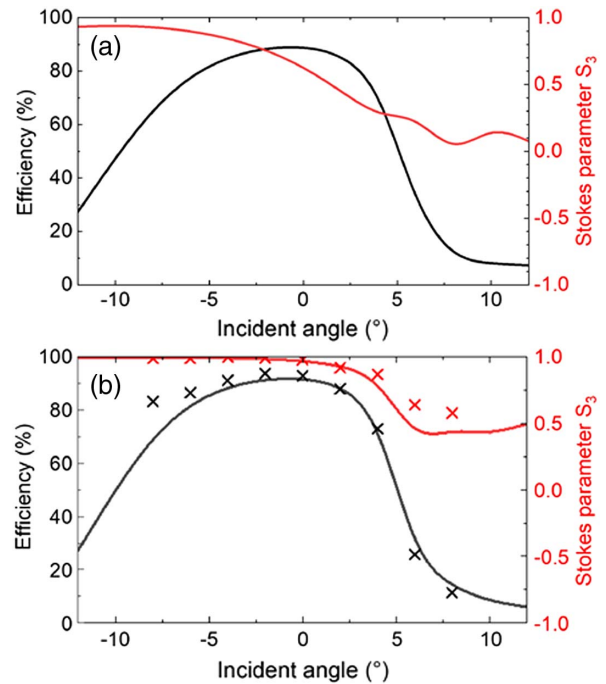

Fig. 6. Angular behavior of optical efficiency and S_3 of a 2.0 µm (a) planar PVG and (b) slanted PVG. The crosses denote the measured results from a 2.0-µm PVG sample.

Fig. 4. Transmittance of a 2.0-µm PVG as a function of input linear polarizer angle.

5(b), we find that the efficiency performance is very similar between slanted and planar configurations at the same thickness. Yet again, the slanted PVG preserves the light at the right-handed circularly polarized state more effectively than does the planar PVG. At regions with low or rapidly changing efficiency, drastic changes in polarization states are observed for both configurations, which is a typical behavior of cholesteric structures [11]. The efficiency and S_3 at different incident angles are shown in Figs. 6(a) and 6(b). Note that the incident angle is defined inside the $n = 1.58$ medium. As the structure is by nature asymmetric (the Bragg plane is tilted along one direction), the angular performance is also asymmetric. Although both PVGs have similar efficiency performance, the planar PVGs deviate more significantly from the circular polarization state compared to the slanted PVGs. The angular efficiency and S_3 responses are also measured for the 2.0-µm PVG sample, and they fit well with the slanted configuration, as Fig. 6(b) shows. This asymmetric behavior also suggests that if PVGs are used as waveguide/light-guide couplers [12], the variation in polarization states at different angles is not negligible, and careful consideration must be taken when utilized in a polarization-sensitive waveguide-coupling scenario.

4. CONCLUSION

Despite the similarity in diffractive efficiency between slanted and planar PVGs, we identified a significant difference in their polarizing properties. The diffracted light from the slanted configuration tends to maintain the circular polarization state, while the planar structure provides more retardance toward the diffracted light. Further experiments using RM257 as reactive mesogen with a relatively small slant angle ϕ ($\sim25°$ in our experiment) reveal that a slanted PVG pattern is preferred for minimizing free energy. This work will also shed light on the optical design of PVG-based waveguide/light-guide couplers.

REFERENCES

1. B. C. Kress and W. J. Cummings, "Towards the ultimate mixed reality experience: HoloLens display architecture choices," SID Symp. Dig. Tech. Pap. **48**, 127–131 (2017).
2. T. Yoshida, K. Tokuyama, Y. Takai, D. Tsukuda, T. Kaneko, N. Suzuki, T. Anzai, A. Yoshikale, K. Akutsu, and A. Machida, "A plastic holographic waveguide combiner for light-weight and highly-transparent augmented reality glasses," J. Soc. Inf. Disp. **26**, 280–286 (2018).
3. Y. Weng, D. Xu, Y. Zhang, X. Li, and S.-T. Wu, "Polarization volume grating with high efficiency and large diffraction angle," Opt. Express **24**, 17746–17759 (2016).
4. J. Kobashi, Y. Mohri, H. Yoshida, and M. Ozaki, "Circularly-polarized, large-angle reflective deflectors based on periodically patterned cholesteric liquid crystals," Opt. Data Process. Storage **3**, 61–66 (2017).
5. Y.-H. Lee, K. Yin, and S.-T. Wu, "Reflective polarization volume gratings for high efficiency waveguide-coupling augmented reality displays," Opt. Express **25**, 27008–27014 (2017).
6. T. Levola, "Novel diffractive optical components for near to eye displays," SID Symp. Dig. Tech. Pap. **37**, 64–67 (2006).
7. T. Rasmussen, "Overview of high-efficiency transmission gratings for molecular spectroscopy," Spectroscopy **29**, 32–39 (2014).
8. F. Bruder, T. Fäcke, R. Hagen, D. Hönel, E. Orselli, C. Rewitz, T. Rölle, and G. Walze, "Diffractive optics with high Bragg selectivity: volume holographic optical elements in Bayfol HX photopolymer film," Proc. SPIE **9626**, 96260T (2015).
9. J. Wang, C. McGinty, J. West, D. Bryant, V. Finnemeyer, R. Reich, S. Berry, H. Clark, O. Yaroshchuk, and P. Bos, "Effects of humidity and surface on photoalignment of brilliant yellow," Liq. Cryst. **44**, 863–872 (2017).
10. X. Xiang, J. Kim, R. Komanduri, and M. J. Escuti, "Nanoscale liquid crystal polymer Bragg polarization gratings," Opt. Express **25**, 19298–19308 (2017).
11. J. L. Fergason, "Cholesteric structure. I. Optical properties," Mol. Cryst. Liq. Cryst. **1**, 293–307 (1966).
12. Y. H. Lee, G. Tan, K. Yin, T. Zhan, and S. T. Wu, "Compact see-through near-eye display with depth adaption," J. Soc. Inf. Disp. **26**, 64–70 (2018).